Progress In Electromagnetics Research C, Vol. 172, 166–173, 2026

PIER C

(Received 3 June 2026, Accepted 19 July 2026, Scheduled 4 August 2026)

A Novel SIW Bandpass Filter Employing Inset and Rectangular-Slot Defects in the Ground Plane

Ramya Natesan and Boopathi Rani Rajasekar*

Department of ECE, National Institute of Technology Puducherry, Karaikal 609609, Puducherry, India

ABSTRACT: This manuscript investigates the design and implementation of a Substrate Integrated Waveguide (SIW) bandpass filter using an inset feed as a defect and a rectangular slot defect in the ground plane. In this research, the feed line is also used as a defect by replicating the inset feed line on the ground. The inset-feed structure on both conducting layers improves filter performance and reduces size. To further enhance the filter's passband characteristics, a simple rectangular slot is introduced in the ground plane. This Defected Ground Structure (DGS) modifies the current distribution and improves the impedance bandwidth. The proposed filter operating at a center frequency of 10.5 GHz with a bandwidth of 500 MHz and offering a return loss better than 30 dB is designed, fabricated, and experimentally validated. The measured results show good agreement with simulations. The filter exhibits good performance, featuring appropriateness for single-channel satellite communication applications.

1. INTRODUCTION

The rapid growth of wireless communication systems demands compact, low-loss, and high-performance microwave filters. Among various microwave filters, bandpass filters (BPFs) are widely used, whose design is complicated compared to low-pass or high-pass filters. Waveguide filters offer low losses, high Q factor, and good power-handling capabilities, and are hence widely utilized despite being bulky and posing difficulty in interconnections. With the advent of planar microwave filters, the disadvantages of waveguide filters were overcome. However, these planar filters suffer from high loss, especially radiation loss, and hence provide a very low Q factor. These limitations led to the development of substrate-integrated waveguide (SIW) filters that offer advantages similar to waveguide filters, such as low losses and good Q factor, while providing easy integration [1–3]. SIW resembles a waveguide because of the presence of lateral vias, which act as side walls. The vias confine the signal and contribute to the reduction of losses and increased Q factor.

Several methods such as the use of metamaterial [4], vias or inductive posts [1, 5, 6], slots [3, 7–9], SIW resonators [2, 8, 10–15], defected microstrip structures (DMS) [16–19], tuning with active/passive components [20,21], defected ground structure (DGS) [2, 4, 19, 22–24], multilayered structures [7, 9, 12, 18, 25], and hybrid structures formed by the combination of them [7–9, 14, 18–21, 26] have been utilized for improving filter characteristics. Slots can be used in applications that require a large bandwidth and improved stopband performance. Vias help suppress spurious signals and harmonics, thereby improving stopband characteristics, but at the cost of additional conductor losses that decrease the filter's quality factor. When multiple resonant cavities are used, coupling between them can be in-line or cross [10]. Improved selectivity can be achieved through transmission zeros by using additional active components like diodes or passive components like capacitors [2], which increase fabrication complexity. A half-mode SIW loaded with S-shaped complementary spiral resonators [27] is also used for introducing transmission zeros (TZs). Recently, controllable TZs have been achieved using hybrid structures comprising microstrip and complementary split-ring resonators (CSRRs) in SIW [28], or DGS along with CSRRs in SIW [34], which increase design complexity. Even though the use of additional active/passive components, multilayered or hybrid structures, improves performance, issues with complexity, fabrication, and alignment increase. Defecting the ground by etching a desired pattern modifies current distribution and alters resonance [19]. Since the SIW structure provides high-pass characteristics, DGS-based SIW filters can be used to improve selectivity by introducing transmission zeroes and suppressing higher-order harmonics. Several shapes of DGS, such as dumbbell [19, 29], modified dumbbell [22, 30], Hilbert curve [24], H-shape [31], and CSRR [4, 28, 32–34], were designed and analyzed in the past; yet simple rectangular slot DGS is not fully explored. Also, the designed filters either provide a wide bandwidth or a narrow bandwidth, which will not serve the purpose. This article presents a novel yet simple bandpass filter structure that offers 500 MHz bandwidth and good passband and stopband characteristics in the X-band, used in satellite and radar applications.

The novelty of the proposed filter lies in the simultaneous utilization of an inset-feed defect and a rectangular-slot defect. Unlike conventional DGS, where resonant slots perturb the ground current, the proposed structure introduces a replicated inset-feed geometry in the ground plane that is identical to

* Corresponding author: Boopathi R. Rajasekar (rbrani@nitpy.ac.in).

the inset feed implemented on the top conductor. This arrangement modifies the coupling mechanism between the microstrip feed and the SIW cavity while simultaneously perturbing the ground-current distribution. Consequently, an additional transmission zero is generated through destructive interference between the direct propagation path and the defect-induced resonant path without increasing structural complexity. Furthermore, a simple rectangular-slot DGS is incorporated to improve passband characteristics. The combination of these two defect mechanisms provides improved selectivity while maintaining a compact single-layer SIW configuration suitable for X-band satellite and radar applications.

The detailed design of the SIW bandpass filter with a DGS structure is presented in Section 2 along with its analysis. Section 3 discusses the electromagnetic behaviour of the proposed filter. Section 4 presents the simulated and measured results, and Section 5 provides the conclusion.

2. DESIGN AND ANALYSIS OF THE SIW BANDPASS FILTER

The structure of the proposed filter is shown in Fig. 1, with its dimensions in mm. The novelty of the design lies in the use of inset-feed ports in the ground plane (GP) in addition to the top plane (TP) and a simple rectangular DGS to improve performance.

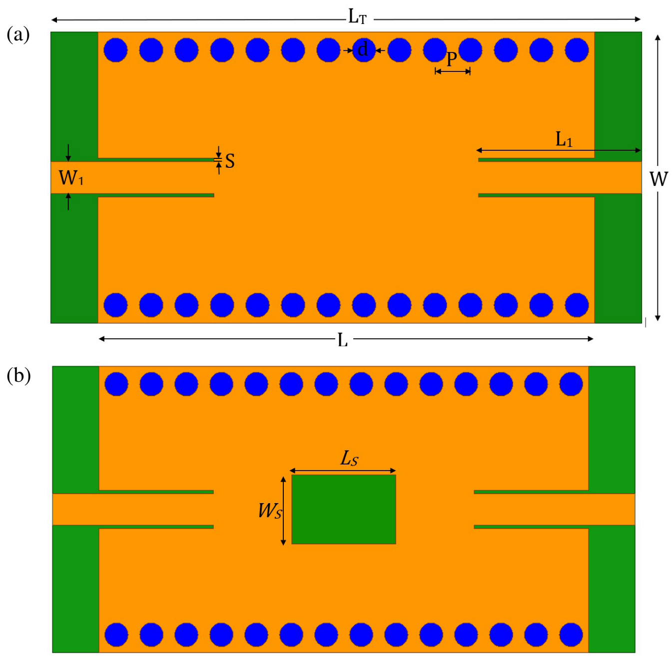

FIGURE 1. (a) Top view of the proposed filter and (b) bottom view of the proposed filter with all the dimensions in mm. ($L_T = 30.25$, $L = 25.42$, $W = 14.5$, $L_1 = 8.349$, $W_1 = 1.565$, $P = 1.815$, $d = 1.21$, $S = 0.4$, $L_s = 5.4$, $W_s = 3.5$).

The design flow of the proposed filter is as follows:

Step a: Design of an SIW high-pass filter.
Step b: Inclusion of an inset-feed structure in the top plane and its replication in the ground plane.
Step c: Rectangular slot DGS and its optimization.

2.1. Design of SIW High Pass Filter (Step a)

Based on the basic SIW design equations, as specified in Equations (1)–(5) [1], the high-pass filter with a cutoff frequency (f_{cm0n}) of 9 GHz is designed. Characteristics of the chosen substrate include a dielectric constant (ϵ_r) of 2, a loss tangent of 0.009, and a height of 0.508 mm.

$$f_{cm0n} = \frac{c}{2\pi\sqrt{\epsilon_r}}\sqrt{\left(\frac{m\pi}{a_e}\right)^2 + \left(\frac{n\pi}{b_e}\right)^2} \quad (1)$$

$$a_e = a - \frac{d^2}{0.95p} \quad (2)$$

$$b_e = b - \frac{d^2}{0.95p} \quad (3)$$

where a_e is the effective width; b_e is the effective length of the SIW cavity, which is obtained from Equations (2) and (3) [1]; a and b define the actual width and length of the SIW structure; and p and d respectively denote the pitch and diameter of the vias. For lateral confinement of the signal, the vias' diameter and pitch are calculated in Equations (4) and (5) [1], respectively.

$$d < 0.2\lambda_g \quad (4)$$

where λ_g is the guide wavelength.

$$p \leq 2d \quad (5)$$

The cutoff frequency of the designed high-pass SIW filter is 9 GHz, as seen from Fig. 2(a). To facilitate providing an input signal to the SIW filter, any one of the feed structures can be used, with the most popular being the microstrip feed, as it provides ease of fabrication and better impedance matching. Microstrip feed structures can be directly coupled, tapered, or inset. Although a tapered feed provides better impedance matching, it obviously increases the size. Circuit size is a very stringent requirement in many applications, and hence, a modified microstrip feed structure, such as an inset feed, is gaining potential. Inset microstrip feed projects itself as a better candidate for narrowband applications as the amount of coupling can be adjusted by varying the inset's gap and depth. Hence, the inset feed is adopted in the proposed SIW filter and is discussed in Step b.

2.2. Inclusion of Inset-Feed Structure in Top Plane and Its Replication in Ground Plane (Step b)

The feed dimensions are given in Fig. 1. The inclusion of an inset feed combines the first two resonant modes, exhibiting band-pass characteristics. To further improve performance, a novel idea of defecting the ground with an inset feed, same as that in the top plane, is used in this design. The replication of the feed in the ground plane defects the ground, resulting in the introduction of a transmission zero, thereby improving filter performance. The characteristic response is shown in Fig. 2(b), which shows a transmission zero at 13 GHz.

The replicated inset structure perturbs both electric- and magnetic-field distributions near the feed transition and introduces an additional resonant path in the ground plane. The

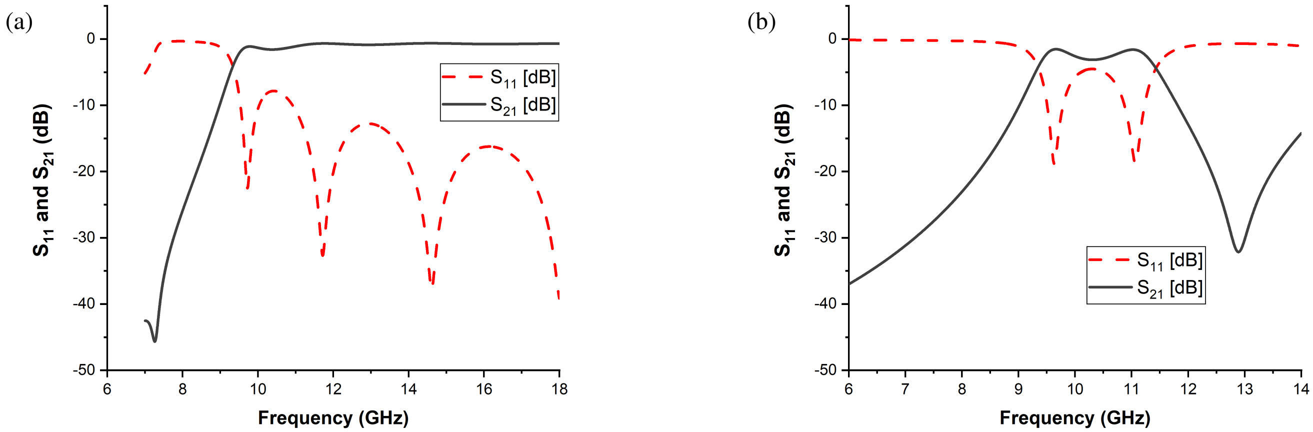

FIGURE 2. (a) Highpass characteristics of the SIW filter and (b) characteristics of the SIW filter with inset-feed in GP and TP.

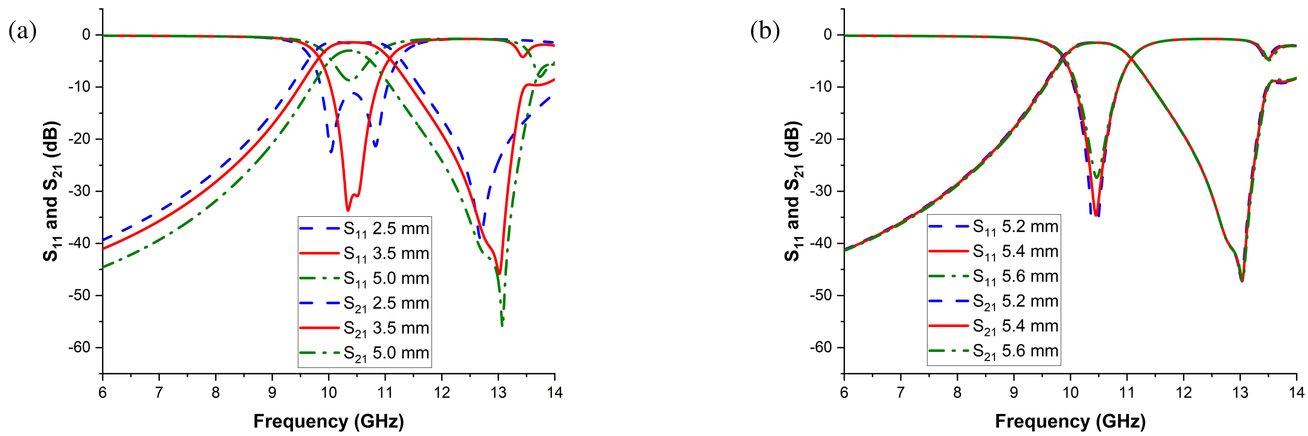

FIGURE 3. Parametric analysis of the slot length (L_s) and width (W_s). (a) Variations of width W_s from 2.5 to 5 mm, with $L_s = 5$ mm and (b) variation of L_s from 5.2 to 5.6 mm with $W_s = 3.5$ mm.

modified current path increases the equivalent inductance and distributed capacitance between the feed and cavity walls. At frequencies close to 13 GHz, the fields associated with this path become out of phase with the dominant transmission mode inside the SIW cavity. The destructive interference between these propagation paths suppresses signal transmission and produces a transmission zero. Consequently, the resonant characteristics of the SIW cavity are modified, producing improved impedance matching and enhanced stopband suppression, but with high insertion loss.

The defect in the ground (feed) improves the filter's passband and stopband responses, but with high insertion loss. From the literature, we understand that using DGS is a simple method to improve filter characteristics. Hence, to further enhance the performance of the proposed filter, an additional DGS is incorporated and discussed in Step c.

2.3. Rectangular Slot DGS and its Optimization (Step c)

This section explores improvements in impedance bandwidth by the inclusion of a rectangular slot in the ground plane. To start with, a square-shaped DGS of 5 mm side length is included at the center of the ground plane. It improves filter performance by better impedance matching at the operating bandwidth. Further, analyses are carried out to finalize optimal dimensions that provide a resonance at the center frequency 10.5 GHz and mirror response from the center frequency. All the prominent variations are illustrated in Figs. 3(a) and 3(b).

To finalize the length (L_s) and width (W_s) of the rectangular slot, parametric analysis is carried out. Initially, the length (L_s) is fixed as 5 mm and width (W_s) varied from 2.5 to 5 mm in steps of 0.5 mm. It is observed that for values of W_s as 2.5 and 3 mm, a wide bandwidth is obtained by combining the first two resonant modes. For W_s between 4 and 5 mm, the bandwidth decreases considerably, but the return loss is not appreciable. Hence, the optimal value of W_s is chosen as 3.5 mm, which provides a passband return loss greater than 30 dB and comparatively better 10 dB impedance bandwidth. Proceeding to optimize the length (L_s), it is varied from 5 to 6 mm by fixing W_s as 3.5 mm. It is observed that as L_s increases, the passband return loss decreases considerably, in addition to a slight decrease in bandwidth. Hence, considering the return loss in the passband to be less than 30 dB, with better passband characteristics, the L_s value is finalized as 5.4 mm. Thus, after a

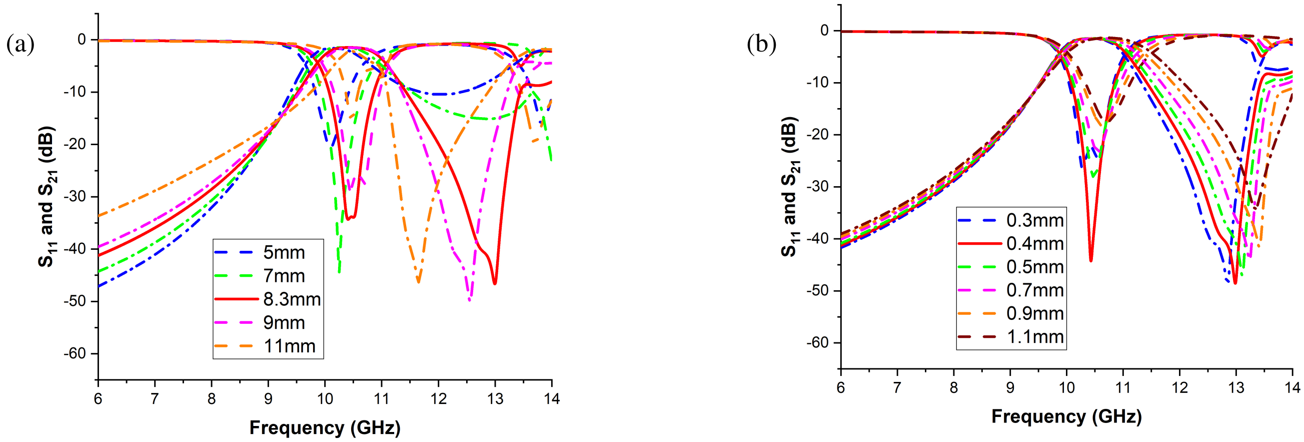

FIGURE 4. Parametric analysis of the inset-feed. (a) Length (L_1) and (b) gap (S).

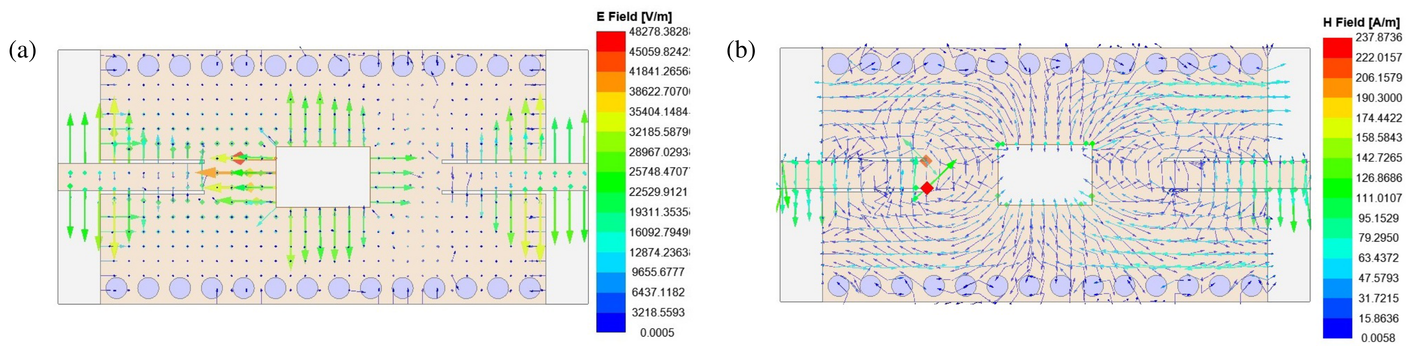

FIGURE 5. Field distribution at resonance. (a) E-field and (b) H-field.

complete analysis of W_s and L_s variations, optimal values are finalized as 3.5 mm and 5.4 mm, respectively, as they provide comparatively good performance in terms of bandwidth, insertion loss, and passband return loss.

2.4. Inset-Feed Optimization

The inset-feed length is denoted as L_1, which consists of a microstrip length 2.42 mm and an inset depth 5.929 mm. To know the impact of inset depth, a parametric analysis is carried out on L_1 by keeping the microstrip length constant, shown in Fig. 4(a). The inset depth primarily controls coupling strength between the feed and the SIW cavity. It impacts input impedance. An increase in inset depth contributes to converging multiple modes and obtains a narrow bandwidth. The S_{21} characteristic is poor for an inset depth less than 8 mm, whereas the S_{11} characteristic deteriorates for an inset depth greater than 9 mm. From these, the inset depth dimension of 8.34 mm is chosen as optimum. An increase in inset gap from 0.3 to 1.1 mm shows a significant increase in bandwidth, while shifting the resonance to the higher end. It governs the impedance matching at the feed transition, shown in Fig. 4(b). Thus, the inset gap dimension of 0.4 mm is chosen as optimum.

3. ELECTROMAGNETIC BEHAVIOUR OF THE PROPOSED FILTER

To study the electromagnetic behaviour of the designed filter, E- and H-fields are plotted in Figs. 5(a) and 5(b), respectively. The electric-field distribution at the centre frequency demonstrates strong field confinement inside the SIW cavity with maximum field intensity around the inset-feed transition. The field concentration indicates efficient excitation of the dominant mode and confirms proper impedance matching. It showcases the E-field predominantly confined to the slot region, while the H-field exhibits symmetric circulating patterns around the resonator. These field distributions confirm the dominant LC resonance and efficient energy confinement at the operating frequency.

Figure 6 illustrates the surface current density at 10.5 GHz and 13 GHz. Strong current concentration around the resonator at 10.5 GHz confirms the passband resonance, whereas the current confinement near the input port at 13 GHz verifies effective stopband suppression, i.e., at the transmission-zero frequency, the electric field becomes localized around the inset-feed-defect region, reducing the field intensity within the main transmission path and preventing signal propagation. This can be evinced from the surface current density plot given in Fig. 6(b).

TABLE 1. Effect of fabrication tolerance on slot dimensions.

Slot Length, L_s (mm)	Slot Length, W_s (mm)	Shift in f_c (MHz)	Change in BW (MHz)	IL (dB)	RL (dB)
5.4	3.3	5	70	1.50	22.7
5.4	3.4	0	40	1.54	26.0
5.4	3.5	0	0	1.54	33.8
5.4	3.6	0	−40	1.54	44.0
5.4	3.7	−5	−90	1.50	27.9
5.2	3.5	0	10	1.47	33.0
5.3	3.5	0	10	1.49	30.0
5.4	3.5	0	0	1.50	34.0
5.5	3.5	5	−30	1.47	57.0
5.6	3.5	10	−40	1.47	40.0

Note: L_s = slot length, W_s = slot width, f_c = center frequency, BW = bandwidth, IL = insertion loss, RL = return loss.

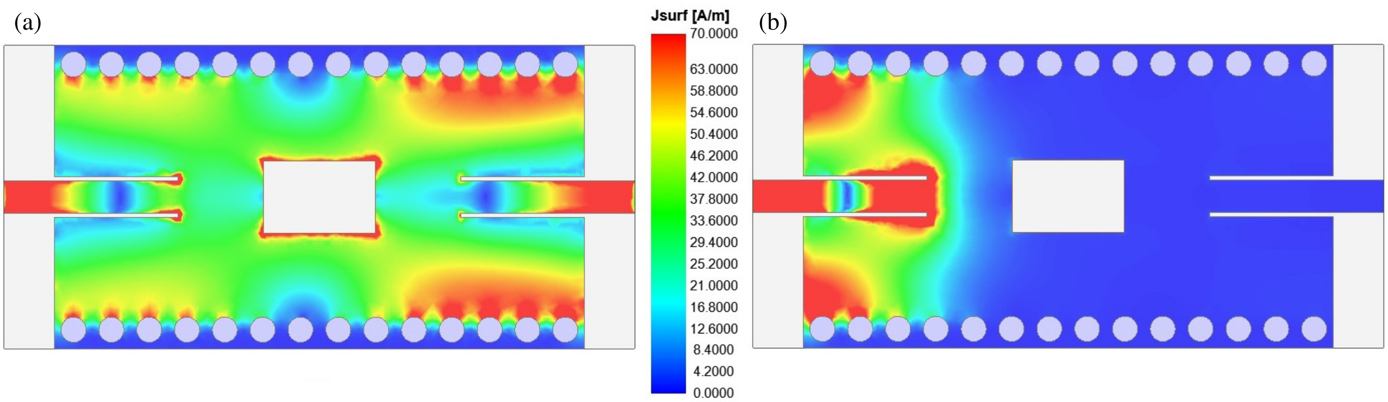

FIGURE 6. Surface current density. (a) At 10.5 GHz and (b) at 13 GHz.

4. RESULTS AND DISCUSSIONS

The proposed filter offers a 3 dB insertion loss and 10 dB impedance band from 10.2 to 10.75 GHz. The proposed filter exhibits a fractional bandwidth (FBW) of approximately 5.25%, corresponding to 550 MHz bandwidth centered at 10.5 GHz. The insertion loss and return loss values of the simulated filter are −1.5 dB and −31 dB, respectively. A transmission zero is obtained at 13 GHz. The loaded quality factor of the proposed filter is 21 as per the ratio of center frequency to the 3 dB pass bandwidth. The unloaded quality factor of the proposed filter is estimated as 104 [32]. The filter offers improved selectivity in the upper passband, with over 20 dB/GHz of selectivity factor, achieved by introducing a TZ using an inset feed DGS and a rectangular-slot DGS. The stopband rejection exceeds 10 dB up to 19.5 GHz, except for a small spurious band near 15 GHz.

To validate the results, the proposed filter is fabricated. Measurement is carried out using a vector network analyzer (VNA). The measurement setup with an image of the prototype is shown in Fig. 7(a). The measured results are on par with the simulated ones, as evident in Fig. 7(b). The measured −10 dB return loss and 3 dB or less insertion loss are from 10.28 to 10.78 GHz, which are close to the simulated results. The slight variations in the measured results might be due to material property variations over frequencies and minor issues in fabrication, such as via filling and soldering. The group delay variation in the passband of the filter is 0.05 ns (violet color line, Y-axis on RHS), which attributes to the optimum performance of the proposed filter.

4.1. Fabrication Tolerance Analysis

4.1.1. Slot Dimensions

The effect of slight variation in the slot dimension during fabrication is analysed in simulation by varying the slot dimensions within ±0.2 mm from the finalized value and provided in Table 1. This reveals that these variations have an impact on the bandwidth and not significantly on the center frequency and insertion loss (IL).

4.1.2. Via Diameter

The effect of slight variation in the via diameter during fabrication is analysed in simulation by varying the via diameter from 1 to 1.4 mm and is provided in Table 2. This reveals that these variations impact the center frequency and not significantly the bandwidth, IL, and return loss (RL).

The comparison between existing literature and the proposed filter is provided in Table 3. The purpose of a filter is to allow

TABLE 2. Effect of fabrication tolerance on via diameter.

Via Diameter, d (mm)	Shift in f_c (MHz)	Change in BW (MHz)	IL (dB)	RL (dB)
1.00	−210	20	1.50	26.80
1.10	−110	0	1.48	32.54
1.20	−10	−20	1.50	48.31
1.21	0	0	1.50	33.80
1.30	100	−30	1.48	33.60
1.40	200	−40	1.48	32.00

Note: d = via diameter, fc = center frequency, BW = bandwidth, IL = insertion loss, RL = return loss. The nominal design corresponds to $d = 1.21$ mm.

TABLE 3. Comparison of the proposed filter with reported SIW bandpass filters.

Ref.	f_c (GHz)	BW (MHz)	FBW (%)	IL (dB)	RL (dB)	TZ	Q_L	Size (mm^2)	Technique/Remarks	Complexity
[6]	10.05	530	5.3	< 2.0	> 18	0	18.9	40.16×17.87	Half-mode SIW. Upper stop-band rejection > 30 dB.	Moderate
[7]	8.5	520	6.1	< 2.5	> 10	2	16.3	20.29×19.37	Multilayer SIW. 50 dB attenuation at TZ.	High
[11]	10.04	420	4.2	NA	> 20	2	23.8	29.5×42	Bypass coupling. > 30 dB stopband attenuation.	High
[12]	10.01	1620	16.2	< 2.0	> 14	0	6.2	11.2×8.57	Shielded SIW. Wide stopband with > 45 dB attenuation at $2.73 f_0$.	Very High
[14]	10.0	100	1.0	NA	NA	2	100	33×25	Parallel-coupled SIW. > 30 dB attenuation in stopband.	Moderate
[15]	11.25	580	5.1	1.55	23	0	19.4	46.31×32.97	Series-connected resonators. Stopband reaches > 20 dB at $1.03 f_0$.	Moderate
[16]	11.5	780	6.8	< 2.0	> 13	2	14.8	24×15	Hybrid SIW. > 40 dB of attenuation in stopband.	High
[17]	9.99	1080	10.8	1.8	20	2	9.3	37.9×20.4	Hybrid SIW. > 20 dB attenuation up to $1.57 f_0$.	High
[18]	10.71	1070	10.0	< 2.0	> 15	2	10.0	23.5×12.6	Multilayer HM-SIW. > 20 dB attenuation in stopband.	Very High
[25]	8.34	824	9.8	1.1	> 10	–	17	27×8.55	Two-layer HMSIW with U-slot slow-wave. Stopband suppression > 30 dB.	High
[26]	10.22	2390	23.4	> 2.5	> 10	0	4.3	30×20	Cascaded SIW. Stopband attenuation > 20 dB.	High
[34]	10.1	2710	26.8	1.5	21	3	3.7	27×22	Hybrid SIW + DGS + DMS. Stopband > 20 dB up to $1.94 f_0$.	High
Proposed	**10.5**	**500**	**4.76**	< 3	> 30	**1**	**21**	**30.25×14.5**	**Inset-fed SIW with rectangular DGS. > 10 dB till $1.87 f_0$. Stopband rejection exceeds 45 dB at 13 GHz.**	**Low**

Note: f_c — center frequency, BW — bandwidth, FBW — fractional bandwidth, IL — insertion loss, RL — return loss; TZ — transmission zeros, QL — loaded quality factor, NA — not available.

only the required band of signals and filter out the other signals. Hence, having a filter passband more than the required bandwidth will not serve the purpose. Most satellite applications need 500 MHz bandwidth to accommodate 1 channel. The filters in [12, 17, 18, 26, 34] provide more than the required bandwidth, which increases system complexity as they offer more than 1 GHz bandwidth. Bandwidth is less than 500 MHz in [11, 14]. Works [6, 7, 11, 15, 16] provide comparable band-

(a)

(b)

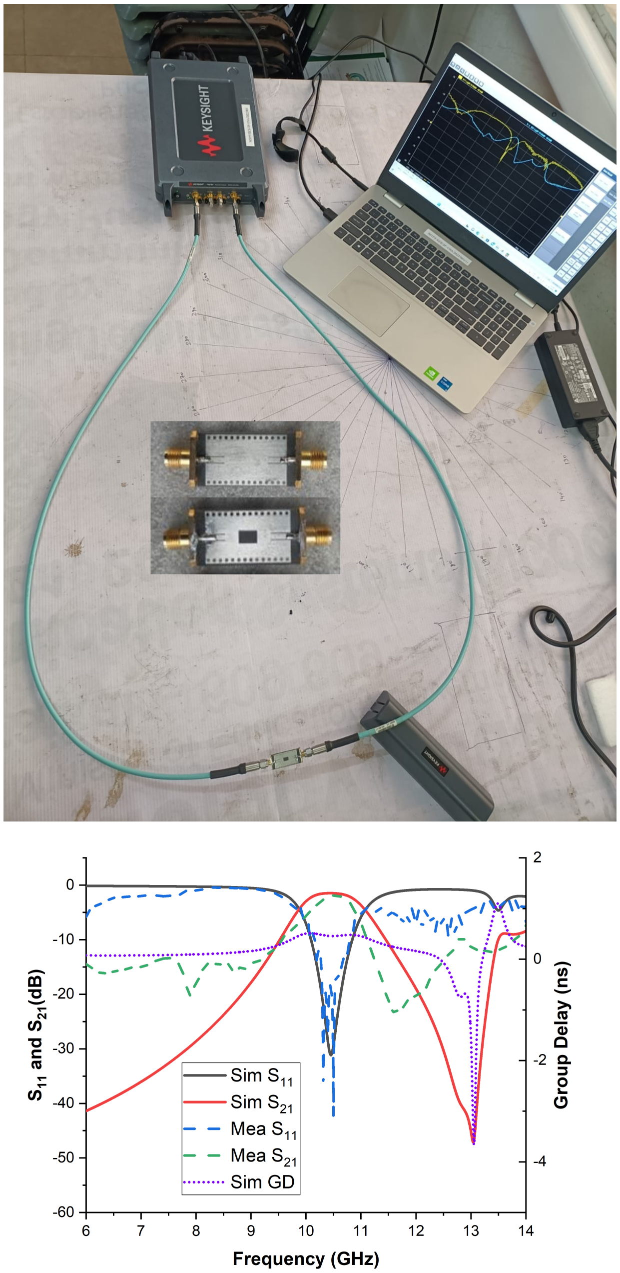

FIGURE 7. (a) Measurement setup and prototype, and (b) simulated and measured results.

width suitable for single-channel communication, but the large circuit area of Refs. [6, 11, 15] is the major drawback compared to our proposed work. The filter in [7] provides the required bandwidth with compact size, but has design complexity as it involves staking layers vertically. Its return loss is high compared to the proposed filter. The reported filters employed techniques such as DMS [16, 17], bypass coupling methods [11], and dual-mode excitation [6], which require relatively complex design approaches. Furthermore, multilayer structures [7, 12, 18, 25] made the system bulky and more difficult to design and align. Ref. [16] offers a slightly higher bandwidth but is complex to design, including more vias, which will increase conductor losses and have moderate return loss. Filters reported in [7, 11, 14, 16–18, 34] offer improved selectivity by generating multiple TZs, but either involve increased design complexity, such as a multilayered architecture, or complex coupling mechanisms, or increased circuit size. Compared to previous studies, the proposed filter is tailored to obtain the required bandwidth of 500 MHz, which meets the application requirement. It features the advantages of a simple structure, a single layer, and is comparatively compact.

Like waveguides, the proposed SIW filter can also be used without restrictions of top and bottom planes, meaning that the slot made in the ground can also be reversed on the patch side, exhibiting invariance in the performance.

5. CONCLUSION

This work has presented a novel idea of using an inset-feed structure in the ground plane as a DGS in addition to a simpler rectangular-slot DGS. Inset feed reduces filter footprint and allows bandwidth tuning by varying inset gap and depth. Defecting the ground plane with the same inset feed helps improve stopband characteristics by the inclusion of a transmission zero. Further, to improve passband characteristics, a simple rectangular-slot DGS is utilized. Parametric analysis on the length and width of the rectangular slot is carried out. Like waveguides, the proposed filter provides the same performance even if the top and bottom planes are reversed. The proposed SIW bandpass filter with 500 MHz bandwidth centered at 10.5 GHz is suitable for single-channel satellite or radar applications operating in the X band.

REFERENCES

[1] Hong, J.-S. and M. J. Lancaster, *Microstrip Filters for RF/Microwave Applications*, John Wiley & Sons, 2004.

[2] Boopathi Rani, R., P. Reshma, and S. Ramkumar, "Substrate-integrated waveguide filters — A review," in *International Conference on Futuristic Communication and Network Technologies*, 603–612, Springer, Singapore, 2020.

[3] Azad, A. R., A. Kumar, D. K. Jhariya, and A. Mohan, "Dual-mode wideband bandpass filter using single SIW cavity with perturbation slot," in *2022 8th International Conference on Signal Processing and Communication (ICSC)*, 108–111, Noida, India, 2022.

[4] Li, W., Z. Tang, and X. Cao, "Design of a SIW bandpass filter using defected ground structure with CSRRs," *Active and Passive Electronic Components*, Vol. 2017, No. 1, 1606341, 2017.

[5] Zhu, F., G. Q. Luo, B. You, X. H. Zhang, and K. Wu, "Planar dual-mode bandpass filters using perturbed substrate-integrated waveguide rectangular cavities," *IEEE Transactions on Microwave Theory and Techniques*, Vol. 69, No. 6, 3048–3057, 2021.

[6] Zhu, F., G. Q. Luo, Z. Liao, X. W. Dai, and K. Wu, "Compact dual-mode bandpass filters based on half-mode substrate-integrated waveguide cavities," *IEEE Microwave and Wireless Components Letters*, Vol. 31, No. 5, 441–444, 2021.

[7] Shen, W. and H.-R. Zhu, "Vertically stacked trisection SIW filter with controllable transmission zeros," *IEEE Microwave and Wireless Components Letters*, Vol. 30, No. 3, 237–240, 2020.

[8] Mishra, G. K., H. K. Pandey, and N. P. Pathak, "A novel SIW bandpass filter design by diagonal coupling approach on single and multilayer model," *AEU — International Journal of Electronics and Communications*, Vol. 200, 155916, 2025.

[9] Yao, Y., G. Dong, Z. Zhu, and Y. Yang, "Stacked arrangement of substrate integrated waveguide cavity-backed semicircle patches for wideband circular polarization with filtering effect," *Frontiers of Information Technology & Electronic Engineering*, Vol. 24, No. 5, 759–766, 2023.

[10] Liu, Q., D. Zhou, Y. Zhang, D. Zhang, and D. Lv, "Substrate integrated waveguide bandpass filters in box-like topology with bypass and direct couplings in diagonal cross-coupling path," *IEEE Transactions on Microwave Theory and Techniques*, Vol. 67, No. 3, 1014–1022, 2019.

[11] Liu, Q., D.-F. Zhou, D.-W. Zhang, and D.-L. Lv, "SIW bandpass filters in modified box-section scheme with bypass/constant/frequency-dependent coupling in diagonal cross-coupling path," *IET Microwaves, Antennas & Propagation*, Vol. 13, No. 5, 559–566, 2019.

[12] "Miniaturized, wide stopband filter based on shielded capacitively loaded siw resonators."

[13] Huang, J.-M., H.-T. Xing, and Z.-H. Ma, "Substrate-integrated waveguide bandpass filter for 5G applications," *Sensors and Materials*, Vol. 36, No. 3, 1105–1113, 2024.

[14] Kiani, S., P. Rezaei, M. Karami, and R. A. Sadeghzadeh, "Substrate integrated waveguide quasi-elliptic bandpass filter with parallel coupled microstrip resonator," *Electronics Letters*, Vol. 54, No. 10, 667–668, 2018.

[15] Dung, K. D., N. D. Tinh, N. T. Hung, and V. T. Hung, "X-band bandpass filter structure for passive radar using SIW technology," *Journal of Military Science and Technology*, Vol. 104, 41–48, 2025.

[16] Lin, G. and Y. Dong, "A compact, hybrid SIW filter with controllable transmission zeros and high selectivity," *IEEE Transactions on Circuits and Systems II: Express Briefs*, Vol. 69, No. 4, 2051–2055, 2022.

[17] Zhu, Y., Y. Dong, J. Bornemann, L. Gu, and D. F. Mamedes, "An inline compact SIW bandpass filter with quasi-elliptic response using microstrip extracted-pole resonators," *IEEE Transactions on Circuits and Systems II: Express Briefs*, Vol. 70, No. 6, 1856–1860, 2023.

[18] Gu, L. and Y. Dong, "Compact half-mode SIW filter with high selectivity and improved stopband performance," *IEEE Microwave and Wireless Components Letters*, Vol. 32, No. 9, 1039–1042, 2022.

[19] Noura, A., M. Benaissa, M. Abri, H. Badaoui, T.-H. Vuong, and J. Tao, "Miniaturized half-mode SIW band-pass filter design integrating dumbbell DGS cells," *Microwave and Optical Technology Letters*, Vol. 61, No. 6, 1473–1477, 2019.

[20] Agasti, R., D. C. Nichols, A. M. Eck, H. H. Sigmarsson, and J. E. Ruyle, "Varactor-tuned superstrate-loaded antenna and filtenna for X-band applications," *IEEE Transactions on Antennas and Propagation*, Vol. 72, No. 10, 7651–7663, 2024.

[21] Paliwal, R., S. Srivastava, and R. Budhiraja, "Customizable substrate integrated waveguide based dual pole band pass filter for X band application," *Progress In Electromagnetics Research M*, Vol. 125, 11–19, 2024.

[22] Liu, C. and X. An, "A SIW-DGS wideband bandpass filter with a sharp roll-off at upper stopband," *Microwave and Optical Technology Letters*, Vol. 59, No. 4, 789–792, 2017.

[23] Huang, T., X. Yang, Y. Huang, Z. He, and Z. Shao, "An X-band SIW-DGS bandpass filter with improved stopband performance," in *2015 IEEE International Conference on Communication Problem-Solving (ICCP)*, 473–474, Guilin, China, 2015.

[24] Chaib, M. E. A., M. Abri, H. A. Badaoui, and N. Cherif, "Bandpass filters based on hybrid structure of substrate integrated waveguide (SIW) and hilbert defected ground structure (HDGS)," *Progress In Electromagnetics Research Letters*, Vol. 104, 27–35, 2022.

[25] Wei, F., X. Y. Wang, H. Y. Kang, B. Li, and D. W. Liao, "Wideband bandpass filter based on U-slotted SW-HMSIW cavities," *International Journal of RF and Microwave Computer-Aided Engineering*, Vol. 28, No. 2, e21178, 2018.

[26] Guvenli, K., S. Yenikaya, and M. Secmen, "Analysis, design, and actual fabrication of a hybrid microstrip-SIW bandpass filter based on cascaded hardware integration at X-band," *Elektronika Ir Elektrotechnika*, Vol. 27, No. 1, 23–28, 2021.

[27] Wei, F., H. J. Yue, J.-P. Song, H. Y. Kang, and B. Li, "Half-mode SIW BPF loaded with S-shaped complementary spiral resonators," *Progress In Electromagnetics Research Letters*, Vol. 77, 13–18, 2018.

[28] Cai, Z.-J., Q. Liu, K. Gong, Y.-L. Zhang, D.-W. Zhang, and D.-F. Zhou, "Compact high-selectivity SIW filter using dual-mode cavity loaded by microstrip and complementary open ring resonators," *IEEE Microwave and Wireless Technology Letters*, Vol. 36, No. 3, 359–362, 2026.

[29] Cherif, N., M. Abri, B. Fellah, J. Tao, and H. Badaoui, "A compact wideband DGS bandpass filter based on half mode substrate integrated waveguide technology," *International Journal of Microwave and Optical Technology*, Vol. 16, No. 2, 142–147, 2021.

[30] Dixit, A., A. Kumar, A. Kumar, and A. Kumar, "Investigation of Substrate Integrated Waveguide (SIW) Filter Using Defected Ground Structure (DGS)," in *Optical and Wireless Technologies: Proceedings of OWT 2019*, Vol. 648, 449–456, Springer, Singapore, 2020.

[31] Nakmouche, M. F., H. Taher, D. E. Fawzy, and A. M. M. A. Allam, "Development of a wideband substrate integrated waveguide bandpass filter using H-slotted DGS," in *2019 IEEE Conference on Antenna Measurements & Applications (CAMA)*, 1–4, Kuta, Bali, Indonesia, 2019.

[32] Soundarya, G. and N. Gunavathi, "Compact dual-band SIW bandpass filter using CSRR and DGS structure resonators," *Progress In Electromagnetics Research Letters*, Vol. 101, 79–87, 2021.

[33] Martinez, J., A. Coves, E. Bronchalo, A. A. S. Blas, and M. Bozzi, "Band-pass filters based on periodic structures in SIW technology," *AEU — International Journal of Electronics and Communications*, Vol. 112, 152942, 2019.

[34] Senathipathi, U. and S. Krishnan, "Compact substrate integrated waveguide bandpass filter with wide stopband tunable transmission zeros," *Electromagnetics*, Vol. 45, No. 7, 526–540, 2025.